RASĀYAN *J. Chem.*
Vol. 19 | No. 4 | 2288-2298 | October-December | 2026
ISSN: 0974-1496 | e-ISSN: 0976-0083 | CODEN: RJCABP
http://www.rasayanjournal.com
http://www.rasayanjournal.co.in

SYNERGISTIC RATE ENHANCEMENT IN MIXED SDS–TRITON X-100 MICELLES FOR THE NUCLEOPHILIC DEACYLATION OF p-NITROPHENYL ACETATE BY TRIETHANOLAMINE: A KINETIC AND REGULAR-SOLUTION INTERACTION STUDY

M. R. Aruna Kumari[1], P. Shyamala[1,✉] D. H. Puranam[2,] K. V. Nagalakshmi[3], and B. Leela Kumari[4]

[1]Department of Chemistry, Andhra University, Visakhapatnam-530017, Andhra Pradesh, India.
[2]Department of Pharmaceutical Sciences, Professor of Practice, Andhra University, Visakhapatnam, Andhra Pradesh, India
[3]Department of Chemistry, Gayatri Vidya Parishad Institute of Higher Learning and Reearch, Visakhapatnam-530048, Andhra Pradesh, India
[4]Department of Chemistry, St. Joseph's College for Women (A), Visakhapatnam-530004, Andhra Pradesh, India
✉Corresponding author: shyamalapulipaka06@gmail.com

ABSTRACT

The kinetics of the nucleophilic deacylation of *p*-nitrophenyl acetate by triethanolamine were investigated in aqueous medium, single-surfactant systems containing sodium dodecyl sulphate (SDS) or Triton X-100 (TX-100), and binary SDS–TX-100 mixed micelles to elucidate the effect of micellar composition on reaction kinetics. Reaction progress was monitored spectrophotometrically under pseudo-first-order conditions by following the formation of *p*-nitrophenolate at 400 nm. Both surfactants enhanced the reaction rate compared with water, with TX-100 exhibiting greater catalytic efficiency. Mixed SDS–TX-100 micelles produced the highest rate enhancement because of synergistic electrostatic and hydrophobic interactions. Regular Solution Theory was applied to evaluate the interaction parameter (β) and the composition-dependent critical micelle concentrations, confirming non-ideal mixed-micelle behaviour. The results demonstrate that mixed micelles provide a tunable reaction microenvironment with superior catalytic performance compared with single-surfactant systems. This study advances the understanding of surfactant-mediated catalysis and provides useful insights for designing efficient aqueous catalytic systems.

Keywords: Micellar Catalysis, Ester Deacylation, Mixed Surfactant Systems, Regular Solution Theory, Reaction Kinetics, Sodium Dodecyl Sulphate, Triton X-100

RASĀYAN *J. Chem.*, Vol. 19, No.4, 2026

INTRODUCTION

Reactions in which nitrophenyl esters transfer their acyl group to a nucleophile remain a central tool for probing mechanisms in both synthetic and biological chemistry. Among these probe esters, p-nitrophenyl acetate is used more often than perhaps any other because its hydrolysis or aminolysis liberates the strongly absorbing p-nitrophenoxide ion, allowing the course of a reaction to be followed continuously by ultraviolet–visible spectroscopy without the need to draw samples or quench aliquots.[1-5] This same sensitivity is what makes p-nitrophenyl acetate a standard substrate for assaying esterase-type enzymes such as acetylcholinesterase, an enzyme central to synaptic signalling, and for evaluating other hydrolytic enzymes involved in lipid turnover and in the breakdown of xenobiotics.[6-9] Its acyl-transfer chemistry has additionally been exploited outside the enzymatic context, for example to track the environmental fate of pesticide residues and industrial contaminants and to characterise esterase-secreting microbial populations relevant to soil and water quality assessment.[10-13] Surfactant self-assembly offers a convenient handle for tuning reaction rates, since the solubilising, concentrating, and charge-screening properties of a micelle can all be adjusted through the choice of surfactant.[4,6-8] Once the surfactant concentration exceeds the critical micelle concentration, monomers aggregate spontaneously into structures possessing a

http://doi.org/10.31788/RJC.2026.1949647
This work is licensed under a CC BY 4.0 license.

hydrophobic interior and a hydrophilic shell, generating a microenvironment reminiscent of the interior of a biological membrane.[14,15] Reactants partition into this assembly, transition states are stabilised, and reactions proceeding through charged or polar pathways are typically accelerated as a result. The pseudophase ion-exchange treatment is the framework most commonly invoked to rationalise these rate changes, attributing them to how substrate and counter-ion binding differ between the aqueous and micellar pseudophases.[16,17] Single-surfactant micelles have been studied extensively enough that their contrasting behaviour is well documented. The anionic head groups of SDS create an interface that repels hydroxide while still concentrating cationic or neutral nucleophiles nearby, whereas the polyoxyethylene shell of the non-ionic surfactant Triton X-100 forms a more hydrated, less charged region that favours partitioning of hydrophobic substrates.[18-21] These contrasting interfacial chemistries carry over into esterolytic kinetics: SDS frequently retards hydrolysis by excluding hydroxide electrostatically, while Triton X-100 can instead favour aminolysis by drawing both substrate and amine together within its palisade layer.[22,23] Combining an ionic surfactant with a non-ionic one to form mixed micelles has drawn growing interest, since such blends can be tuned to physicochemical properties unattainable with either component alone.[24-26] Mixing alters the critical micelle concentration, the net surface charge, the aggregation number, and the degree of interfacial hydration, and the resulting cooperativity between dissimilar head groups can improve substrate solubilisation while shifting the polarity of the reaction zone. Regular-solution theory captures the extent of this non-ideal mixing through an interaction parameter, beta, which measures whether the two surfactants attract or repel one another within the aggregate.[27,28] SDS/Triton X-100 mixtures in particular are known to lower the electrostatic potential at the interface and to loosen the packing there, conditions favourable for reactions that depend on a balance of hydrophobic and electrostatic contributions.[29,30] Triethanolamine combines nucleophilic character with hydrogen-bond donor/acceptor capacity through its three hydroxyl arms, properties that have made it a widely used reagent in aminolysis and transesterification chemistry.[31-34] Because it is amphiphilic, it partitions readily between the bulk aqueous phase and a micellar pseudophase, allowing it to act either as a direct nucleophile or as a general base catalyst depending on the local environment. Pairing triethanolamine with p-nitrophenyl acetate therefore constitutes a convenient, well-characterised model system for examining how organised media modulate acyl-transfer chemistry involving a hydrophobic ester and a water-soluble amine. The present investigation compares the kinetics of this ester–amine reaction in water, in single-component SDS and Triton X-100 micelles, and in their binary mixtures, with the aim of relating micellar composition and interfacial architecture to the observed aminolysis rate. Contrasting the normal (single-surfactant) and mixed systems provides a route to disentangling the hydrophobic, electrostatic, and hydrogen-bonding contributions operating at the micelle–water interface, insight that is relevant both to modelling enzyme-like catalysis in self-assembled systems and to designing greener, more efficient aqueous reaction media. This objective aligns with Sustainable Development Goal 12 (Responsible Consumption and Production), which calls for the environmentally sound management of chemicals throughout their life cycle.

EXPERIMENTAL

Material and Methods

p-Nitrophenyl acetate, triethanolamine, sodium dodecyl sulphate (SDS), and Triton X-100, all of analytical reagent grade, were used directly as received without further purification. Stock solutions of each reagent were prepared using double-distilled water and were kept in amber bottles to protect them from light-induced degradation. Ionic strength across all solutions was held constant with sodium perchlorate, and every aqueous solution was prepared from water of specific conductivity below 1×10^{-6} Scm^{-1}.

General Procedure

Kinetic runs on the deacylation of p-nitrophenyl acetate by triethanolamine were carried out under pseudo-first-order conditions in water, in SDS, in Triton X-100, and in mixed SDS/Triton X-100 media. Each run was started by rapidly adding a small volume of the ester stock solution to a reaction mixture already containing triethanolamine, surfactant, and sodium perchlorate at the temperature of interest, held

constant by a thermostatted water bath (±0.1 °C). Triethanolamine was always present in large excess over the ester to preserve pseudo-first-order behaviour. Pseudo-first-order rate constants were extracted from linear plots of the natural logarithm of ($A_\infty - A_t$) against time; each reported value is the average of no fewer than three independent runs, reproducible to within ±4%.

Detection Method

Reaction progress was monitored spectrophotometrically on a Shimadzu UV-1800 double-beam spectrophotometer fitted with matched 1 cm quartz cells, by tracking the rise in absorbance of the p-nitrophenolate chromophore at 400 nm, the wavelength at which this species absorbs most strongly, allowing continuous, non-destructive measurement of the reaction without sample withdrawal.

Preparation of Mixed Micelles and Calculation of Interaction Parameters (β)

Binary micellar systems combining SDS and Triton X-100 were prepared to probe how micellar composition governs the ester–amine reaction. The target mole fraction of Triton X-100 in the feed, α(TX-100), was set by combining calculated volumes of pre-standardised sodium dodecyl sulphate and Triton X-100 stock solutions in double-distilled water, with the total surfactant concentration in every mixture kept above the critical micelle concentration of the corresponding blend so that micellisation was complete. Mixtures were equilibrated at the working temperature for at least thirty minutes before any kinetic measurement, ensuring the surfactants were homogeneously distributed. Critical micelle concentrations for pure SDS, pure Triton X-100, and their blends were obtained by the surface-tension method under the same ionic strength and temperature used in the kinetic work. The experimentally measured mixed critical micelle concentration, C_{MIX}, was compared with the value predicted for ideal mixing by the Clint equation, and the extent of departure from ideality was expressed through the regular-solution interaction parameter β:

$$\beta = \frac{\ln(\alpha_1 C_{MIX} / X_1 C_1)}{(1-X_1)^2}$$

where C1 denotes the critical micelle concentration of Triton X-100 taken alone, CMIX is the critical micelle concentration of the blend, X_1 and X_2 (with $X_2 = 1 - X_1$) are the mole fractions of Triton X-100 and SDS within the micelle, and α1 is the stoichiometric (feed) mole fraction of Triton X-100. A dedicated FORTRAN routine, listed in full as Supplementary Information at the end of this manuscript, was written to solve the regular-solution relations iteratively from the experimental critical micelle concentration data and the feed mole fractions until both β and the micellar composition (X_1, X_2) converged. The resulting β values were related to the kinetic results to distinguish synergistic from antagonistic surfactant behaviour: a positive β signals repulsion between the two surfactants, while a negative value points to attractive, synergistic mixing. Monomer concentrations of each surfactant at equilibrium were likewise back-calculated from the total surfactant concentration and the measured C_{MIX}, and these values were fed into the subsequent analysis of how kobs depends on micellar composition.

Determination of Mixed-Micelle Composition

Micellar composition and the interaction parameter β were obtained using the Rubingh regular-solution formalism, taking the surface-tension-derived C_{MIX} values as input and solving the Rubingh relation numerically for X_1 (the micellar mole fraction of Triton X-100), with $X_2 = 1 - X_1$ giving the SDS fraction. β followed directly from the regular-solution expression once X_1 was known. All non-linear solving was carried out with an in-house FORTRAN implementation of a Newton–Raphson iteration, initiated at $X_1(0) = \alpha 1$ and continued until $|\Delta X_1|$ fell below 1×10^{-6}. The same routine returned the monomer concentrations and monomer fractions fi at the point of micellisation, together with intermediate diagnostic output; the complete source code and a representative output file are reproduced as Supplementary Information at the end of the manuscript.

RESULTS AND DISCUSSION

Kinetics in Aqueous Medium

Deacylation of p-nitrophenyl acetate by triethanolamine was first examined in plain water under pseudo-first-order conditions ([ester] = 8.0×10^{-5} mol dm^{-3}, [amine] = 2.0×10^{-2} mol dm^{-3}, ionic strength 0.1 mol dm^{-3} maintained with sodium perchlorate, 301 ± 0.1 K), following the rise in absorbance of the p-

nitrophenolate ion at 400 nm. Plots of $\ln(A_\infty - A_t)$ against time were linear throughout, consistent with first-order behaviour in the ester, and the rate rose in direct proportion to the amine concentration, confirming a first-order dependence on the nucleophile as well. Such a dependence is consistent with a bimolecular (SN^2-type) substitution in which the hydroxyl oxygen of triethanolamine attacks the carbonyl carbon of the ester, forming a tetrahedral transition state whose collapse cleaves the ester linkage to release p-nitrophenol together with a short-lived O-acylated amine intermediate (Scheme-1). Adding sodium perchlorate produced essentially no change in the rate constant, showing that the rate-determining step involves only neutral species and that transition-state stabilisation in water is not electrostatically driven.

Kinetics in SDS and Triton X-100 Micellar Media

The same reaction was then examined in SDS and in Triton X-100 under otherwise identical conditions. Surface-tension measurements gave critical micelle concentrations of 2.6×10^{-3} mol dm^{-3} for SDS and 0.48×10^{-3} mol dm^{-3} for Triton X-100, values consistent with earlier reports.[30] Rate constants were measured while varying the ester concentration at fixed amine concentration and vice versa, with surfactant concentration and ionic strength held constant. A first-order dependence on both reactants persisted in both micellar media, indicating that the underlying mechanism is unchanged from the aqueous case (Table-1, Figure-1). Increasing surfactant concentration from 0.0 to 80.0×10^{-3} mol dm^{-3} (Figure-2) raised the rate constant steadily to a maximum of 14.53×10^{-5} s^{-1}in sodium dodecyl sulphate (at 8.0×10^{-3} mol dm^{-3}) and 36.3×10^{-5} s^{-1} in Triton X-100 (at 4.0×10^{-3} mol dm^{-3}), beyond which a modest decline set in, most plausibly because saturation of the micelle limits further access of the substrate. The initial rise reflects co-solubilisation of both the ester and the amine within the micelle, where reduced local polarity favours nucleophilic attack; the later decline is consistent with over-packing and compartmentalisation of the reactants at high surfactant loading, which lowers their effective collision frequency at the reactive interface. Triton X-100 outperformed sodium dodecyl sulphate roughly threefold under matched conditions, a gap traced to their differing interfacial chemistry: the less charged, more hydrophobic palisade of Triton X-100 accommodates both the neutral ester and the hydrophilic amine more readily, whereas the negatively charged sodium dodecyl sulphate interface can electrostatically repel the partially protonated amine and hinder its approach to the ester carbonyl. Collectively, these findings confirm that micelles behave as micro-reactors that reshape the local reaction environment without changing the underlying SN^2-type pathway, with catalytic performance governed chiefly by how effectively the micelle co-solubilises both reactants and balances interfacial polarity against compactness. This contrast between the anionic and non-ionic single-surfactant systems sets the stage for examining the cooperative or antagonistic behaviour expected when the two surfactants are combined, a topic taken up in the following section.

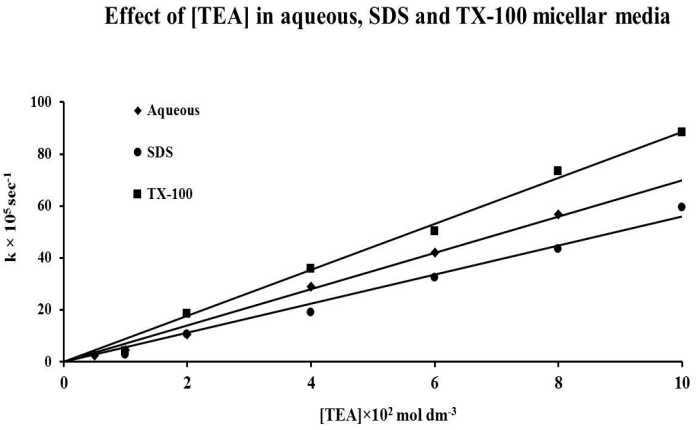


Fig.-1: Rate constant ($k \times 10^5$ s^{-1}) as a function of triethanolamine concentration in water and in SDS and TX-100 media. [Ester] = 8×10^{-5} mol dm^{-3}, [SDS] = [TX-100] = 4×10^{-3} mol dm^{-3}, μ = 0.1 mol dm^{-3}, T = 301 ± 0.1 K

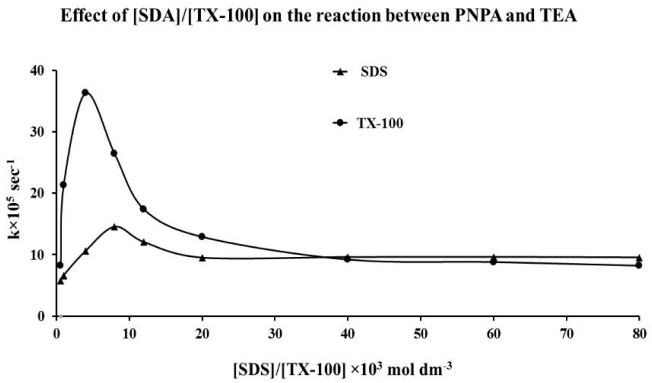


Fig.-2: Dependence of the Observed Rate Constant (kobs) on SDS and TX-100 Concentration for the Deacylation of p-nitrophenyl Acetate by Triethanolamine. [Ester] = 8.0×10^{-5} mol dm^{-3}; [Amine] = 2×10^{-2} mol dm^{-3}; μ = 0.1 mol dm^{-3}; T = 301 ± 0.1 K.

Product Formation and Stoichiometry

Reaction stoichiometry was established spectrophotometrically by the mole-ratio method in both water and the micellar media. Ester concentration was fixed at 8.0×10^{-5} mol dm^{-3} while the amine concentration was varied in the presence of 0.1 mol dm^{-3} sodium dodecyl sulphate or Triton X-100, and product absorbance at 400 nm was recorded after 24 hours. A one-to-one stoichiometry between the ester and the amine emerged in every medium, consistent with clean formation of p-nitrophenol (Fig.-3). Although triethanolamine carries three hydroxyl groups, only one engages in acylation under these conditions, a restriction attributable to steric hindrance once the first substitution has occurred, to the reduced reactivity of the remaining hydroxyls once electron density has been withdrawn, and to confinement effects within the micelle that limit access to additional reactive sites. Kinetic and thermodynamic factors together favour a single, stable mono-acylated product forming within the timeframe of the experiment.

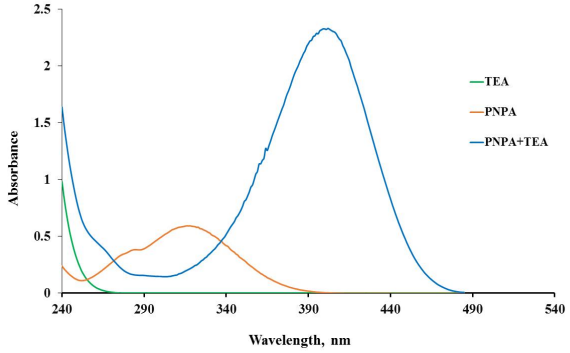
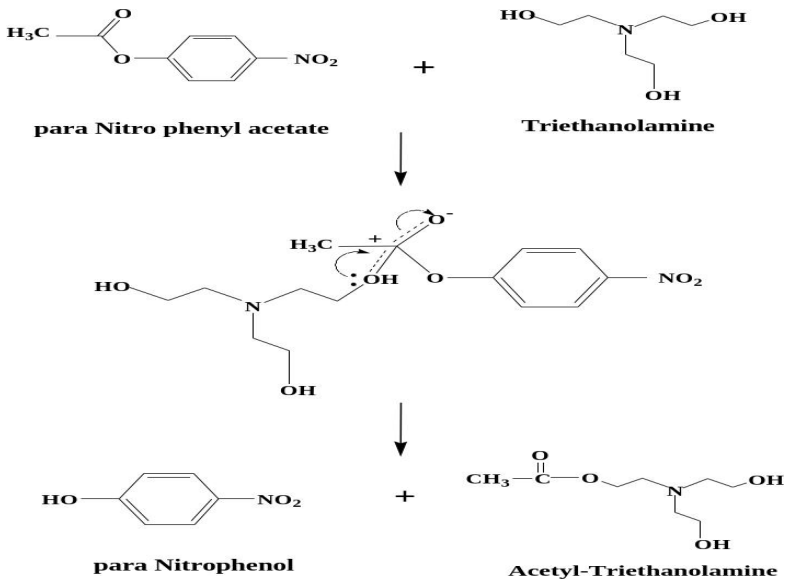


Fig.-3: UV–visible Spectra of the Ester, the Amine, and their Reaction Mixture in Water, Showing the Characteristic P-Nitrophenol Absorption Band Near 400 nm

Mechanistic Interpretation

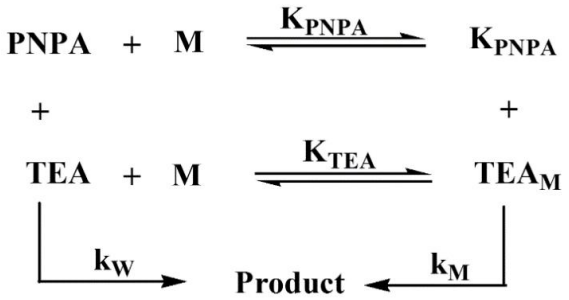
The overall transformation is a nucleophilic deacylation that yields the chromogenic product p-nitrophenol, and the first-order dependence on both reactants in every medium is consistent with a single SN^2-type pathway throughout. Triethanolamine attacks the carbonyl carbon of the ester to form a tetrahedral intermediate whose breakdown releases p-nitrophenoxide (subsequently protonated to p-nitrophenol) together with a transient O-acylated amine. Micelles accelerate this chemistry by concentrating both reactants at the interface, stabilising the developing transition state, and providing a microenvironment conducive to nucleophilic attack. The two surfactants reach their peak rate enhancement at different concentrations, reflecting their distinct interfacial architectures, yet the mechanism and first-order kinetics remain the same across every medium studied (Scheme-1).



Scheme-1: Proposed Mechanistic Pathway for the Interaction of Triethanolamine with p-nitrophenyl Acetate

Kinetic Model in Micelles

At constant ionic strength (0.1 mol dm^{-3} sodium perchlorate), the deacylation reaction is markedly faster in the presence of either surfactant, and both rate–concentration profiles show the biphasic shape characteristic of micellar catalysis: the rate constant climbs with surfactant concentration, peaks, and then falls off. The position and height of this maximum differ between the two surfactants, reflecting their distinct micellar environments. As the aggregation number grows, the local concentration of triethanolamine near the interface is expected to rise as well; electrostatic attraction between surfactant head groups and the nucleophile's counter-ions raises its effective local concentration, while incorporation of the ester into the micelle similarly boosts its effective concentration. Together, this dual enrichment at the interface accounts for the observed rate acceleration, on the premise that the reactive ester group sits close to the nucleophile at the micelle–water boundary, within what is generally termed the Stern layer. Past a certain surfactant loading, the rate falls again, most likely because less substrate remains available within the micellar pseudophase at that point. In broad terms, the nucleophilic reaction rate is set by how strongly the substrate associates with the micelle hydrophobically and by how strongly the anionic nucleophile is drawn electrostatically into the interfacial zone. For sodium dodecyl sulphate, the hydrophobic ester favours the micellar core while the amine sits mainly at the micelle water boundary; this spatial separation concentrates both reactants in a confined region and favours a productive orientation for nucleophilic attack, so the rate climbs sharply with surfactant concentration up to a maximum near the critical micelle concentration, where solubilisation of the ester and interfacial accumulation of the amine are both optimal. Beyond that point, further micelle formation over-compartmentalises and dilutes the reactants within an expanding pseudophase, lowering their encounter frequency and causing the rate to fall. Triton X-100 behaves differently. Its polyoxyethylene chains create a polar, hydrogen-bonding shell that concentrates both reactants while stabilising the developing charge in the transition state, and hydrogen bonding between the amine and the ether oxygens of the surfactant raises the electron density on nitrogen, enhancing its nucleophilicity. As a result, the rate rises more gradually with Triton X-100 concentration and does not show a sharp peak right at the critical micelle concentration; instead, it continues climbing past that point to a maximum near 0.004 mol dm^{-3} before eventually declining as the enlarged micellar phase dilutes the reactants. The peak rate reached in Triton X-100 substantially exceeds that in sodium dodecyl sulphate, reflecting the combined benefits of more efficient solubilisation, stronger transition-state stabilisation, and enhanced nucleophile activation offered by the non-ionic interface. The deacylation of p-nitrophenyl acetate by triethanolamine in the presence of a micelle is summarised in Scheme-2.



Scheme-2: Reaction between p-nitrophenyl Acetate and Triethanolamine in the Presence of a Micelle

Table-1: Effect of Ester, Amine, and Ionic-Strength Concentration on the Rate of Reaction in Aqueous and SDS/TX-100 Micellar Media

[SDS] = [TX-100] = 4 × 10^{-3} mol dm^{-3}; T = 301 ± 0.1 K.

[PNPA]×10^5 mol dm^{-3}	[TEA]×10^2mol dm^{-3}	$NaClO_4$ mol dm^{-3}	Aqueous k×10^5 s^{-1}	SDS k×10^5 s^{-1}	TX-100 k×10^5 s^{-1}
4.0	2.0	0.1	9.45	10.61	36.71
8.0	2.0	0.1	10.56	10.52	36.37
12.0	2.0	0.1	9.95	10.71	35.63
16.0	2.0	0.1	10.14	11.29	36.17
20.0	2.0	0.1	10.14	10.94	36.48
4.0	2.0	0.2	9.54	10.58	36.72
4.0	2.0	0.4	9.62	10.43	36.69
4.0	2.0	0.8	9.59	10.62	36.64
4.0	2.0	1.0	9.47	10.46	36.77
8.0	0.5	0.1	2.32	-	-
8.0	1.0	0.1	4.61	2.69	16.41
8.0	2.0	0.1	10.56	10.52	35.87
8.0	4.0	0.1	28.78	18.84	60.72
8.0	6.0	0.1	42.12	32.22	83.21
8.0	8.0	0.1	56.84	43.47	117.8
8.0	10.0	0.1	68.77	59.53	139.6

Kinetics in Mixed SDS–Triton X-100 Micellar Media

Blends of an anionic and a non-ionic surfactant often depart from ideal mixing in ways that pure-component measurements alone cannot reveal, whether through synergism or antagonism. Determining the micellar composition (Xi) and the interaction parameter β connects this thermodynamic non-ideality to the kinetic changes actually observed, separating the contribution of altered reactant binding from any change in the intrinsic reactivity within the micelle.

Calculation and Definitions

The experimental mixed critical micelle concentration at each feed composition α was fed into the Rubingh formalism to obtain the micellar mole fractions X_1 (Triton X-100) and X_2 (sodium dodecyl sulphate), with β following from equation (1), in which C_1 is the critical micelle concentration of pure Triton X-100:

$$\beta = \frac{\ln(\alpha_1 C_{MIX}/X_1 C_1}{(1-X_1)^2} \qquad (1)$$

The monomer fraction remaining unassociated at the onset of micellisation for each surfactant (f_1, f_2) and the corresponding monomer concentrations were obtained from a mass balance evaluated at C_{MIX}. These non-linear relations were solved numerically with the FORTRAN routine given as Supplementary

Information, whose output underlies the mixed-micellar parameters gathered in Table-2, namely C_{MIX}, the ideal critical micelle concentration for comparison, the micellar mole fractions X_1 and X_2, β, the monomer fractions f_1 and f_2, and the monomer concentrations themselves.

Table-2: Compositional Parameters of SDS–TX-100 Mixed Micelles

Mole fraction TX-100	Exp. CMC ×10³ mol dm⁻³	Ideal CMC ×10³ mol dm⁻³	X_1	X_2	β	f_1	f_2	C_1-mon ×10³	C_2-mon ×10³	C_{Tot}-mon ×10³
0.0	2.60	-	-	-	-	-	-	-	-	-
0.2	0.86	1.381	0.539	0.461	-1.915	0.665	0.574	0.172	0.688	0.860
0.4	0.67	0.939	0.670	0.330	-1.684	0.833	0.469	0.268	0.402	0.670
0.6	0.39	0.712	0.687	0.313	-3.500	0.710	0.192	0.234	0.156	0.390
0.8	0.18	0.573	0.666	0.334	-7.167	0.450	0.041	0.144	0.036	0.180
1.0	0.48	-	-	-	-	-	-	-	-	-

Experimental and ideal CMC, micellar mole fractions (Xi), interaction parameter β, monomer fractions (fi), and monomer concentrations (T = 301 K). Note: the Rubingh mixed-micelle equations were solved with the FORTRAN routine provided at the end of this manuscript; convergence details are given in the Supplementary Information.

Micellar Composition and Interaction Parameters

Applying the Rubingh formalism to the mixed-micelle data returns interaction parameters that are consistently negative, ranging from β = −1.68 to −7.17, a clear signature of synergism between Triton X-100 and sodium dodecyl sulphate. This negative value grows in magnitude as the Triton X-100 feed fraction rises, reaching its most negative point at α = 0.8, indicating that non-ideal stabilisation of the mixed aggregate strengthens as Triton X-100 content increases. Throughout the composition series, the micellar mole fraction of Triton X-100 (X_1) stays below its corresponding feed value of 0.539 at α = 0.2 and between 0.666 and 0.687 across α = 0.4–0.8, showing that sodium dodecyl sulphate is preferentially drawn into the mixed micelle. The proportion of Triton X-100 remaining as free monomer falls sharply as α rises, pointing to strong incorporation of Triton X-100 into the micellar interior, while the total micellised surfactant concentration increases steadily with total surfactant loading, consistent with progressively more efficient aggregation. Together, these observations suggest that sodium dodecyl sulphate supplies the structural framework of the mixed micelle while Triton X-100 contributes stabilising interactions that ease head group repulsion and improve hydrophobic packing. The marginally higher critical micelle concentration recorded for pure Triton X-100 (α = 1.0) relative to α = 0.8 falls within normal experimental scatter and should be read alongside its associated uncertainty.

Pseudophase Kinetic Analysis

The standard pseudophase treatment, linking the observed rate constant (kobs) to rate constants in the aqueous and micellar phases via equation (2), was applied to the kinetic data:

$$\frac{1}{\left(k_{obs} - k_w\right)} = \frac{1}{k_m} + \frac{1}{k_m K_a}\left(\frac{1}{C_M}\right) \qquad (2)$$

Here kw is the aqueous rate constant, km the rate constant within the micellar pseudophase, Ka the substrate–micelle association (binding) constant, and CM the concentration of micellised surfactant ($C_M = C_{TOT} - CMC_{mix}$). Plotting $1/(k_{obs} - k_w)$ against $1/C_M$ gave a linear relationship in every case, and km and Ka were obtained from the resulting slope and intercept (Table-4). The binding constant K_a peaks at α = 0.2 (33.53 × 10²) and falls steadily as the Triton X-100 fraction rises, reaching 2.09 × 10² at α = 0.8, showing that substrate binding to the micelle is strongest when the surface is dominated by anionic sodium dodecyl sulphate (Fig.-4). The intramicellar rate constant km moves in the opposite direction, rising steadily from 2.11 × 10^{-4} to 47.25 × 10^{-4} as α increases to 0.8 before falling back to 16.73 × 10^{-4} for pure Triton X-100. This steady rise up to α = 0.8 shows that the micellar microenvironment becomes an

increasingly favourable setting for the chemical step itself as Triton X-100 content grows, since its non-ionic character improves substrate orientation and stabilises the transition state, thereby promoting intramicellar catalysis.

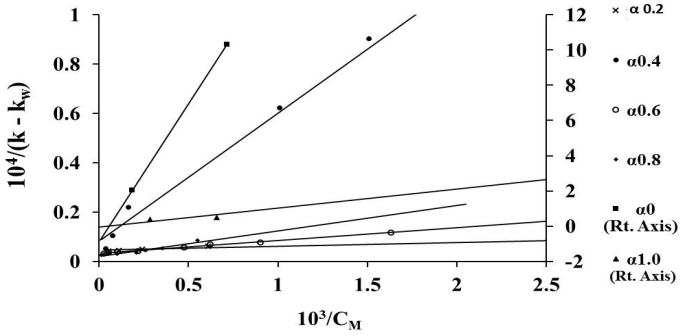


Fig.-4: Linear Plots of $1/(k_{obs} - k_w)$ against $1/C_M$ for the different Triton X-100 Mole Fractions Studied

Table-3: Effect of Total SDS/TX-100 Concentration and Triton X-100 Mole Fraction on the Rate of Reaction
[Ester] = 8.0×10^{-5} mol dm^{-3}, [Amine] = 2.0×10^{-2} mol dm^{-3}, μ = 0.1 M ($NaClO_4$), T = 301 K

[SDS]×10³ mol dm⁻³	α=0.0	α=0.2	α=0.4	α=0.6	α=0.8	α=1.0
0.4	0.26	3.22	5.57	9.4	12.74	0.41
0.6	0.57	6.56	8.51	13.78	19.53	0.82
0.8	0.61	7.6	10.7	15.32	23.47	1.26
1.0	0.66	11.4	13.6	18.94	28.41	2.13
2.0	0.85	16.9	19.3	24.57	32.68	2.97
4.0	1.057	21.3	24.8	26.83	34.77	3.63
8.0	1.453	23.2	27.1	28.15	37.21	2.64
16.0	1.13	25.6	29.4	31.71	40.83	1.54

Table-4: Pseudophase-Derived Parameters: Binding Constant (Ka) and Intramicellar Rate Constant (km) Obtained from Linear Fits of $1/(k_{obs} - k_w)$ vs $1/C_M$ for each α

αTX-100	$K_a \times 10^{-2}$ (dm³ mol⁻¹)	$k_m \times 10^4$ (s⁻¹)
α=0.0	0.554	2.11
α=0.2	33.53	21.24
α=0.4	11.89	26.21
α=0.6	6.22	31.63
α=0.8	2.09	47.25
α=1.0	0.58	16.73

Correlation of Observed Rate Constants with Micellar Parameters

Observed rate constants rise with both total surfactant concentration and the Triton X-100 feed fraction, culminating in a maximum at α = 0.8. At low Triton X-100 content (α = 0.2) the large K_a values show that substrate binding and partitioning into the micelle dominate the rate; at higher Triton X-100 fractions, however, the sharp increase in k_m indicates that intramicellar reactivity takes over as the principal driver of the enhancement (Table-3). Partitioning, governed by K_a, therefore contributes most at low micellar concentration, while intramicellar reactivity, governed by k_m, controls the kinetics once the Triton X-100 fraction is high. The cooperative pairing of charged sodium dodecyl sulphate head groups with the bulky polyoxyethylene chains of Triton X-100 creates an interfacial environment optimised for both substrate binding and catalytic turnover, and this dual contribution underlies the pronounced synergism seen throughout the mixed-micelle system. Overall, mixed sodium dodecyl sulphate–Triton X-100 micelles show clear synergism (negative β), preferential incorporation of sodium dodecyl sulphate, and rate behaviour that depends strongly on composition. At low α, catalysis is driven mainly by substrate binding (K_a); at high α, intramicellar reactivity (k_m) takes over; and the mixture at α = 0.8 offers the most efficient catalytic environment of the series, striking the best balance between electrostatic and non-ionic

stabilisation within the mixed aggregate. Because this enhancement is achieved entirely in aqueous media, without added organic solvents, the approach directly supports the resource-efficient, environmentally sound chemical practice targeted by Sustainable Development Goal 12.

CONCLUSION

Deacylation of p-nitrophenyl acetate by triethanolamine is accelerated substantially by micellar media relative to water, with the rate enhancement, at optimum concentration, following the order mixed sodium dodecyl sulphate–Triton X-100 > pure Triton X-100 > pure sodium dodecyl sulphate, corresponding to roughly forty-fold, four-fold, and two-fold accelerations over the aqueous reaction, respectively. Pseudophase analysis shows that the binding constant Ka is largest at $\alpha = 0.2$, where reactant binding is maximal, while the intramicellar rate constant km rises with Triton X-100 fraction and peaks at $\alpha = 0.8$. These findings demonstrate that the mixed micellar system achieves synergistic catalysis by pairing efficient reactant accumulation, contributed by sodium dodecyl sulphate, with enhanced intrinsic reactivity, contributed by Triton X-100. The resulting cooperative environment, in which the electrostatic stabilisation of sodium dodecyl sulphate combines with the compact hydrophobic character of Triton X-100, delivers the greatest rate enhancement observed in this study and establishes the mixed micelle as a particularly effective micro reactor for this ester–amine system, consistent with the synergistic behaviour predicted by the negative β values and in contrast with reports for single-surfactant systems.[6,7,9,22]

By operating entirely in water and avoiding organic co-solvents, this mixed-micellar strategy for accelerating ester aminolysis offers a practical, environmentally benign route relevant to Sustainable Development Goal 12 (Responsible Consumption and Production), supporting the sound, resource-efficient management of chemical reactions.

ACKNOWLEDGMENTS

P. Shyamala gratefully acknowledges the continued support and encouragement extended by Andhra University. K. V. Nagalakshmi likewise thanks G.V.P. College of Engineering for institutional support.

CONFLICT OF INTERESTS

The authors declare that there is no conflict of interest.

AUTHOR CONTRIBUTIONS

The present work is related to *SDG-12: Responsible Consumption and Production*. All the authors contributed significantly to this manuscript, participated in reviewing/editing and approved the final draft for publication. The research profile of the authors can be verified from their ORCID ids, given below:

M. R. Aruna Kumari https://orcid.org/0000-0002-3478-5016
P. Shyamala https://orcid.org/0000-0001-8271-2607
Deva H. Puranam https://orcid.org/0000-0002-2941-4085
K. V. Nagalakshmi https://orcid.org/0000-0002-2779-4707
B. Leela Kumari http://orcid.org/0000-0001-7623-3343

Open Access: This article is distributed under the terms of the Creative Commons Attribution 4.0 International License (http://creativecommons.org/licenses/by/4.0/), which permits unrestricted use, distribution, and reproduction in any medium, provided you give appropriate credit to the original author(s) and the source, provide a link to the Creative Commons license, and indicate if changes were made.
Cite this article as: R. A. Kumari *et al.*, *Rasayan J. Chem.*, 19(4), 2288-2298(2026), https://doi.org/10.31788/RJC.2026.1949647

REFERENCES

1. H. Gutfreund and J. M. Sturtevant, *Biochemical Journal*, **63**, 656(1956), https://doi.org/10.1042/bj0630656
2. F. J. Kezdy and M. L. Bender, *Biochemistry,* **1**, 1097 (1962), https://doi.org/10.1021/bi00912a021
3. Hua, R. H. Hoechemer and M. R. Hoffmann, *The Journal of Physical Chemistry*, **99**, 2335(1995), https://doi.org/10.1021/j100008a015
4. Z. Huang, S. Cheng and X. Zeng, *Journal of Dispersion Science and Technology*, **24**, 213(2003), https://doi.org/10.1081/DIS-120019972

5. M. Cuccovia, E. H. Schroeter, P. M. Monteiro and H. Chaimovich, *Journal of Organic Chemistry*, **43**, 2248(1978), https://doi.org/10.1021/jo00405a034
6. L. García-Río, J. C. Mejuto and M. Pérez-Lorenzo, *Journal of Colloid and Interface Science,* **301**, 624 (2006), https://doi.org/10.1016/j.jcis.2006.05.037
7. E. Fernández, L. García-Río, J. R. Leis, J. C. Mejuto and M. Pérez-Lorenzo, *New Journal of Chemistry*, **29**, 1594(2005), https://doi.org/10.1039/b507190a
8. L. García-Río, J. C. Mejuto and M. Pérez-Lorenzo, *New Journal of Chemistry*, **28**, 988(2004), https://doi.org/10.1039/b401226g
9. S. K. Verma and K. K. Ghosh, *Colloids and Surfaces A: Physicochemical and Engineering Aspects*, **368**, 154 (2010), https://doi.org/10.1016/j.colsurfa.2010.07.030
10. L.S.Romsted, *The Journal of Physical Chemistry* B, **116**, 13966(2012), https://doi.org/10.1016/j.molliq.2013.11.022
11. N. Suzuki, *Applied Chemistry*, **4**, 1 (2024), https://doi.org/10.3390/appliedchem4010001
12. S. Ahuja, S. Jain and S. P. Moulik, *Langmuir*, **21**, 8355(2005), https://doi.org/10.1021/la051509g
13. M. Pisarcik, F. Devínsky and I. Lacko, *Colloids and Surfaces A: Physicochemical and Engineering Aspects,* **436**, 416 (2013), https://doi.org/10.1016/S0927-7757(00)00589-6
14. S. S. Rawat, S. Mukherjee and A. Chattopadhyay, *The Journal of Physical Chemistry B*, **101**(10), 1922(1997), https://doi.org/10.1021/jp962736h
15. A. Ali, N. A. Malik, U. Farooq, S. Tasneem and F. Nabi, *Journal of Surfactants and Detergents*, **19**, 527(2016), https://doi.org/10.1007/s11743-016-1800-4
16. S. P. Moulik, A. K. Rakshit and B. Naskar, *Journal of Surfactants and Detergents,* **27**, 895 (2024), https://doi.org/10.1002/jsde.12757
17. A. L. Bose, D. Bhattacharjee and D. Goswami, *Colloids and Surfaces B: Biointerfaces*, **209**, 112193(2022), https://doi.org/10.1016/j.colsurfb.2021.112193
18. B. Mirgorodskaya, F. G. Valeeva, R. A. Kushnazarova, S. S. Lukashenko and L. Y. Zakharova, *Kinetics and Catalysis*, **62,** 82(2021), https://doi.org/10.1134/S0023158420060099
19. S. Mujeeb and A. M. Khan, *Journal of Environmental Chemical Engineering,* **13**, 118649 (2025), https://doi.org/10.1016/j.jece.2025.118649
20. D. Tikariha Jangde, A. Sinha and B. Kumar, *International Journal of Chemical Kinetics*, **57**, 12(2025), https://doi.org/10.1002/kin.70014
21. R. Sarkar, K. Karmakar, S. M. Rahaman, S. Kundu, A. Pal, A. Rakshit and B. Saha, *Journal of Molecular Liquids,* **395,** 123847(2024), https://doi.org/10.1016/j.molliq.2023.123847
22. L. García-Río, J. C. Mejuto and M. Pérez-Lorenzo, *Chemistry – A European Journal,* **11**, 4361 (2005), https://doi.org/10.1002/chem.200401067
23. N. J. Naso, F. A. Bellesi, V. M. P. Ruiz-Henestrosa and A. M. Pilosof, *Food Research International,* **161**, 111804(2022), https://doi.org/10.1016/j.foodres.2022.111804
24. K. S. Shukla, P. C. Mathur and O. P. Bansal, *Journal of Inorganic and Nuclear Chemistry,* **35,** 1301 (1973), https://doi.org/10.1016/0022-1902(73)80203-9
25. M. D. La Rubia, R. Pacheco, A. Sánchez, A. B. López García, S. Sánchez and F. Camacho, *International Journal of Chemical Reactor Engineering,* **10,** 1(2012), https://doi.org/10.1515/1542-6580.3023
26. S. Y. Horng and M. H. Li, *Industrial & Engineering Chemistry Research,* **41**, 257(2002), https://doi.org/10.1021/ie0106711
27. R. K. Padhy and S. Sahu, Monatshefte für Chemie – Chemical Monthly, 153, 69(2022), https://doi.org/10.1007/s00706-021-02874-9
28. S. G. de Ávila, M. A. Logli and J. R. Matos, *International Journal of Greenhouse Gas Control***, 42,** 666(2015), https://doi.org/10.1016/j.ijggc.2015.10.001
29. T. L. Donaldson and Y. N. Nguyen, *Industrial & Engineering Chemistry Fundamentals*, **19**, 260(1980), https://doi.org/10.1021/i160075a005
30. A. B. Mirgorodskaya, F. G. Valeeva, R. A. Kushnazarova, S. S. Lukashenko and L. Y. Zakharova, *Kinetics and Catalysis,* **62**, 82(2021), https://doi.org/10.1134/S0023158420060099

[RJC-9647/2026]